

Electronic Supplementary Information (ESI)

Mixed-valent neptunium oligomer complexes based on cation-cation interactions

Sebastian Schöne, Juliane März, Thorsten Stumpf and Atsushi Ikeda-Ohno*

*Helmholtz-Zentrum Dresden-Rossendorf (HZDR), Institute of Resource Ecology,
Bautzner Landstraße 400, 01328 Dresden, Germany*

(* E-mail: a.ikeda@hzdr.de or ikeda.atsushi16@jaea.go.jp)

Contents

1. Synthesis.....	3
1-1. Np(IV) tetrachloride.....	3
1-2. $[\{\text{Np}^{\text{IV}}\text{Cl}_4\}\{\text{Np}^{\text{V}}\text{O}_2\text{Cl}(\text{THF})_3\}_2]\cdot\text{THF}$ (THF = tetrahydrofuran) (1).....	3
1-3. $[\{\text{Np}^{\text{IV}}\text{Cl}_3\}\{\text{Np}^{\text{V}}\text{O}_2(\mu_2\text{-Cl})(\text{THF})_2\}_3\{\mu_3\text{-Cl}\}]$ (2)	3
2. Characterisation.....	5
2-1. Single-crystal X-ray diffraction (SC-XRD).....	5
2-2. Nuclear magnetic resonance (NMR) spectroscopy	5
2-3. Infrared (IR) spectroscopy	6
2-4. UV-visible-NIR absorption spectroscopy.....	6
2-5. Powder X-ray diffraction (PXRD).....	6
3. Experimental data	7
3-1. Microscopic images.....	7
3-2. Structure drawing of reported compounds.....	8
3-2-1. Trinuclear complex.....	8
3-2-2. Tetranuclear complex.....	9
3-3. Bond valence sum (BVS) calculation	10
3-4. NMR spectroscopy.....	11
3-5. IR spectroscopy	13
3-6. UV-visible-NIR absorption spectroscopy.....	14
3-7. PXRD	17
3-8. Crystallographic data	19
References	20

1. Synthesis

Caution! Neptunium (^{237}Np) is a radioactive nuclide and, therefore, precautions with suitable equipment and a facility for radiation protection are required for handling this radionuclide. All the experiments using ^{237}Np were carried out in a controlled laboratory at the Institute of Resource Ecology, Helmholtz-Zentrum Dresden-Rossendorf, Germany.

1-1. Np(IV) tetrachloride

The starting compound of Np(IV) tetrachloride was prepared from NpO_2 according to the synthetic procedure to prepare UCl_4 ¹ with slight modification. 100 mg of NpO_2 was first dissolved in 2.0 ml of concentrated nitric acid (HNO_3) and the resultant suspension was stirred with a magnetic stirrer for 4 hours under a reflux condition. This process converts NpO_2 into $\text{NpO}_2(\text{NO}_3)_2 \cdot n\text{H}_2\text{O}$ with dark-red colour. The sample was then evaporated at $\sim 420\text{ K}$ ($150\text{ }^\circ\text{C}$) for 12 hours to yield a purple solid product. No further drying was performed, meaning that the obtained purple solid product ($\text{NpO}_2(\text{NO}_3)_2 \cdot n\text{H}_2\text{O}$) was not a completely dried solid. The resultant solid compound of Np(VI) nitrate was then transferred into 5.0 ml of hexachloropropene (C_3Cl_6) and refluxed at $\sim 490\text{ K}$ ($220\text{ }^\circ\text{C}$) under an inert atmosphere for 12 hours. This heating process in hexachloropropene leads to the reduction of Np(VI) to -(IV) and the chlorination simultaneously, resulting in the production of Np(IV) tetrachloride compounds as brownish precipitate. The resultant precipitate was then decanted under an inert atmosphere to separate from the solvent, washed the precipitate with dichloromethane (dried and stored over MgCl_2) four times, and dried at $\sim 340\text{ K}$ ($70\text{ }^\circ\text{C}$) for 30 minutes under an inert atmosphere to evaporate the remaining dichloromethane as much as possible. An orange-brown solid was obtained as a final product. All the chemicals (except NpO_2) used in this study were analytical grade or higher, and used without further purification.

As also discussed in the main text, it is difficult to accomplish 100% reduction from Np(VI) to -(IV) with the current synthetic route based on the simultaneous reduction and chlorination in hexachloropropene. As a result, the final product of Np(IV) tetrachloride always contains a small amount of Np(V) chlorides (as neptunyl(V)) as impurity. The synthesised Np(IV) tetrachloride compound is extremely sensitive to moisture and air and, therefore, it is practically difficult to perform powder X-ray diffraction measurements on the synthesised compound to confirm the formed phase(s) and to estimate the amount of Np(V) impurity. The compound was found to be decomposed in ~ 5 min even with a specially made air-tight sample holder.

1-2. $[\{\text{Np}^{\text{IV}}\text{Cl}_4\}\{\text{Np}^{\text{VO}_2}\text{Cl}(\text{THF})_3\}_2] \cdot \text{THF}$ (THF = tetrahydrofuran) (**1**)

A 9 mg of Np(IV) tetrachloride (Batch **A**) was suspended in 0.5 ml of THF- d_8 and the sample mixture was stirred for 3 days under an inert atmosphere. The resultant supernatant was separated from a solid residue by centrifuge and slowly evaporated, yielding compound **1** as a crystalline solid (1.6 mg). The obtained crystalline material was used for single-crystal X-ray diffraction, whilst the solid residue from the original sample mixture (7.4 mg) was characterised by PXRD and IR spectroscopy.

1-3. $[\{\text{Np}^{\text{IV}}\text{Cl}_3\}\{\text{Np}^{\text{VO}_2}(\mu_2\text{-Cl})(\text{THF})_2\}_3\{\mu_3\text{-Cl}\}]$ (**2**)

A 18 mg of Np(IV) tetrachloride (Batch **B**) was mixed with 1 mL of THF- d_8 and the resultant suspension was stirred for 5 days under an inert atmosphere. The supernatant was then separated from a solid residue by centrifuge and further decanted. Slow evaporation of the decanted solution yielded a crystalline material (10.5 mg) that was found to contain compound **2**

as a major phase with a minor presence of **1** and additional unidentified phases (Fig. S11). The obtained crystalline material was used for single-crystal X-ray diffraction, whilst the solid residue from the original sample mixture (7.0 mg) was characterised by PXRD and IR spectroscopy.

2. Characterisation

2-1. Single-crystal X-ray diffraction (SC-XRD)

Crystals of compounds **1** and **2** were analysed at 100 K on a Bruker D8 Venture single-crystal X-ray diffractometer equipped with micro-focused Mo K α radiation ($\lambda = 0.71073 \text{ \AA}$) and a PHOTON 100 CMOS detector. Single crystals appropriate for the measurement were selected on an optical microscope equipped with a polarization filter, and the selected crystals were mounted on a MicroMount™ supplied by MiTeGen, USA, with mineral oil. Several sets of narrow data frames were collected with generic φ - and ω -scans. The collected data were treated with the Bruker APEX3 program suite including the Bruker SAINT software package for integration.² Empirical absorption correction using the multi-scan method (SADABS)³ was applied to the collected data. The structure was solved and refined with full-matrix least-squares data on F^2 using the Bruker SHELXTL⁴ software package and the program ShelXle.⁵ All non-hydrogen atoms were refined anisotropically. Hydrogen atoms of THF molecules were placed at calculated positions and allowed to ride on their parent atoms.

There is significant residual electron density remaining in the provided crystallographic data (.cif file) for compound **2**. The collected frames and the integration procedure were carefully examined, and several sets of frames were collected from several different crystals and analysed. However, none of them could solve the remaining residual electron density. The diffraction data from this best crystal did not reach the resolution of 0.84 \AA and showed relatively broad reflections that are caused by the high mosaicity of the crystal. These facts cause the difficulty in searching for a possible twin law, which could potentially lead to better agreement factors. It was possible to process the collected diffraction data with the resolution of 0.84 . However, this resulted in worse agreement factors ("CCDC1884778_Tetramer_HigherRes.cif") as compared with the results from lower resolution ("CCDC1884778_Tetramer.cif"). The data were also carefully examined in the reciprocal space, but it was not successful in identifying a possible twin matrix. Additionally, there are three big electron density peaks remaining in close proximity to the Np positions. The structure solution was carefully examined in several different space groups. However, all the attempts led to the same residual electron densities. We presume that these residual densities stem from partial disorder of the molecule itself with a $\sim 180^\circ$ rotation on the axis perpendicular to the Np1-C17 line. This would result in the residual electron densities around the Np atoms Np1~Np4 (Np1-Q4; Np2-Q2; Np4-Q1; Np3-Q3) and, hence, lower the agreement factors. Several attempts were made to model this disorder. None of these attempts succeeded in appropriately modelling the disorder of the whole molecule, but only the heavy Np atoms could be split into two parts and could be placed on the residual electron densities, which is presumably due to the low resolution. However, given the plate like shape of the polynuclear Np complex with the THF molecules located in the equatorial plane of the neptunyl unit and the hydrogen bond acceptors (O and Cl) in the axial position, such a disorder could occur on the analysed crystal. The provided .cif file for **2** is the best data that we could accomplish.

2-2. Nuclear magnetic resonance (NMR) spectroscopy

NMR spectra were recorded on a Varian Inova 400 spectrometer with a ^1H frequency of 399.89 MHz. All spectra were recorded at 298 K with a Varian PFG ID probe head with z gradient. THF- d_8 with 0.03% TMS was purchased at Deutero GmbH.

2-3. Infrared (IR) spectroscopy

IR spectra of the samples yielding the compounds **1** and **2** (both solid phase and supernatant) were measured on an Agilent Cary 630 FT-IR spectrometer equipped with a single-reflection attenuated total reflection (ATR) accessory made of diamond. The measurements were performed in an oxygen- and water-free glove box filled with N₂. The spectra were recorded between 4000 and 650 cm⁻¹ with a resolution of 2 cm⁻¹.

2-4. UV-visible-NIR absorption spectroscopy

UV-visible absorption spectra of the supernatants of the sample mixtures yielding compounds **1** and **2** were recorded on a J&M Analytik AG TIDAS 100 spectrometer equipped with optical fibres with a 1 cm optical path length. The measurements were performed in an oxygen- and water-free glove box filled with N₂. The spectra were recorded between 200 and 1025 nm.

2-5. Powder X-ray diffraction (PXRD)

Bulk solid samples containing the compounds **1** and **2** were characterised by powder X-ray diffraction. The data were collected at ambient temperature on a Rigaku MiniFlex 600 equipped with Cu K α radiation ($\lambda = 1.54184 \text{ \AA}$) and a D/Tex Ultra Si strip detector in the Bragg–Brentano geometry (θ – 2θ mode). The samples were mounted on a zero-background Si sample holder basement (cut of (911) orientation) under an oxygen- and water-free atmosphere and the basement was further covered with a specially made air-tight sample holder, which keeps the water-free and inert atmosphere during the PXRD measurements.

3. Experimental data

3-1. Microscopic images

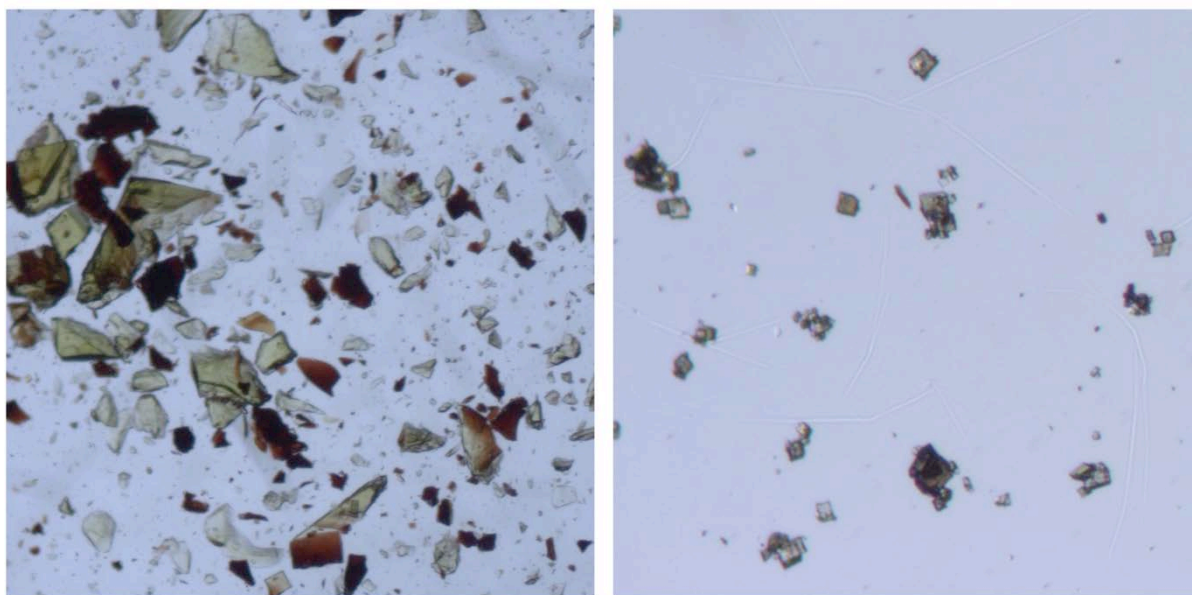


Figure S1. Optical microscopic images of single crystals of **1** (left) and **2** (right).

3-2. Structure drawing of reported compounds

3-2-1. Trinuclear complex

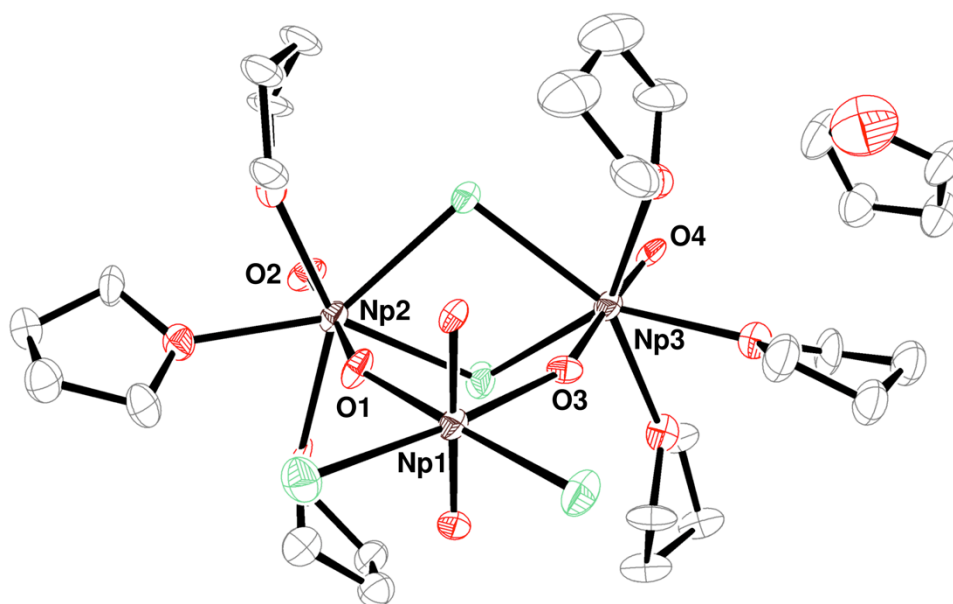


Figure S2. ORTEP representation of the mixed-valent Np(V/VI) trinuclear complex, $[\{Np^{VI}O_2Cl_2\}\{Np^{V}O_2Cl(THF)_3\}_2]\cdot THF$.⁶ Thermal ellipsoids are drawn at 50% probability level and hydrogens are omitted for clarity. Colour code: carbon (C, grey), chlorine (Cl, light green), oxygen (O, red) and neptunium (Np, dark brown).

3-2-2. Tetranuclear complex

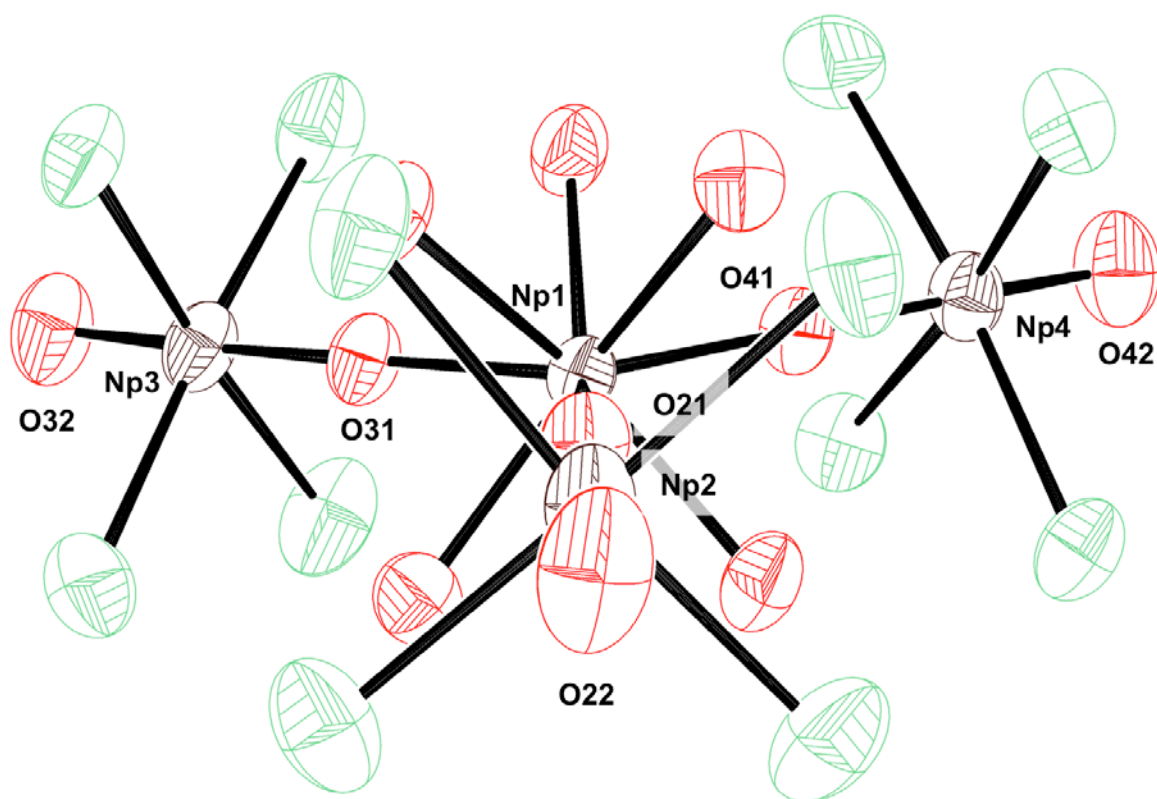


Figure S3. ORTEP representation for the mixed-valent Np(IV/V) tetranuclear unit, $[\text{Np}^{\text{IV}}(\text{Np}^{\text{V}}\text{O}_2)_3(\text{H}_2\text{O})_6\text{Cl}_{12}]^{5-}$ in the compound $[\text{BuMeIm}]_5[\text{Np}(\text{NpO}_2)_3(\text{H}_2\text{O})_6\text{Cl}_{12}]$.⁷ Thermal ellipsoids are drawn at 50% probability level and hydrogens are omitted for clarity. Colour code: chlorine (Cl, light green), oxygen (O, red) and neptunium (Np, dark brown).

Table S1. Selected bond distances (Å) and bond angles (°) for the trinuclear Np(IV/V) complex **1** and the reported trinuclear Np(V/VI) complex⁶

Distance / Å			Angle / °		
Np(IV/V) trimer (1)		Np(V/VI) trimer [Ref 6]	Np(IV/V) trimer (1)		Np(V/VI) trimer [Ref 6]
Np1-O1	2.249	2.303	O1-Np2-O2	176.65	176.34
Np1-O3	2.270	2.316	O3-Np3-O4	177.33	176.84
Np2-O1	1.918	1.912	L1-Np1-L2*	178.20	178.15
Np2-O2	1.793	1.804			
Np3-O3	1.911	1.885			
Np3-O4	1.794	1.752			
Np1-Np2	4.084	4.105			
Np1-Np3	4.089	4.108			
Np2-Np3	4.298	4.340			

* "L" stands for the linearly arranged Cl atoms (Cl1 and Cl2) and neptunyl(VI) oxygen atoms (O3 and O4) for **1** and the Np(V/VI) complex, respectively.

Table S2. Selected bond distances (Å) and bond angles (°) for the pseudo-tetrahedral tetranuclear Np(IV/V) complex **2** and the reported planar tetranuclear Np(IV/V) complex⁷

Distance / Å		Distance / Å		Angle / °		Angle / °	
Np(IV/V) tetramer (2)		Np(IV/V) tetramer [Ref 7]		Np(IV/V) tetramer (2)		Np(IV/V) tetramer [Ref 7]	
Np1-O1	2.177	Np1-O21	2.299	O1-Np2-O2	178.35	O21-Np2-O22	179.16
Np1-O3	2.264	Np1-O31	2.307	O3-Np3-O4	175.61	O31-Np3-O32	178.12
Np1-O5	2.252	Np1-O41	2.258	O5-Np4-O6	175.8	O41-Np4-O42	178.75
Np2-O1	1.957	Np2-O21	1.884				
Np2-O2	1.744	Np2-O22	1.800				
Np3-O3	1.886	Np3-O31	1.873				
Np3-O4	1.818	Np3-O32	1.788				
Np4-O5	1.907	Np4-O41	1.902				
Np4-O6	1.785	Np4-O42	1.784				

3-3. Bond valence sum (BVS) calculation

Bond valence sum values (V) of an i atom can be calculated according to the following equation;⁸

$$V_i = \sum_{j=1}^N \exp[(R_{ij}^0 - R_{ij})B]$$

where N is the total coordination number in the primary coordination sphere of the i atom, j is the coordinating atoms around the i atom, R_{ij} is the experimentally determined bond distance between the i and j atoms. R_{ij}^0 is called the bond valence parameter and is obtained through a systematic analysis of relevant crystal structure data, whilst B is an empirically determined parameter. The primary coordination sphere of Np atoms in compounds **1** and **2** consists only of Np–O and Np–Cl. For the Np^V-O bond distance, several R_{ij}^0 and B values were reported by different researchers.⁹⁻¹¹ The V values listed in Tables 1 and 2 in the main text were obtained by applying these different R_{ij}^0 and B values to the Np^V-O bond. All other parameters were taken from a literature by Zachariasen.¹²

3-4. NMR spectroscopy

It is important to confirm the purity of the solvent used for the syntheses of **1** and **2**, particularly in order to identify the origin of oxygen source to generate neptunyl units from the Np(IV) source. Shown in Figures S4 and S5 are the ^1H -NMR spectra for the supernatants of the sample mixtures yielding compounds **1** and **2**. The water impurity in THF- d_8 should generate a peak at around 2.46 ppm.¹³ The collected NMR spectra show, however, no significant peak in the relevant region, confirming that the THF used for the syntheses was water-free, at least in terms of NMR spectroscopy.

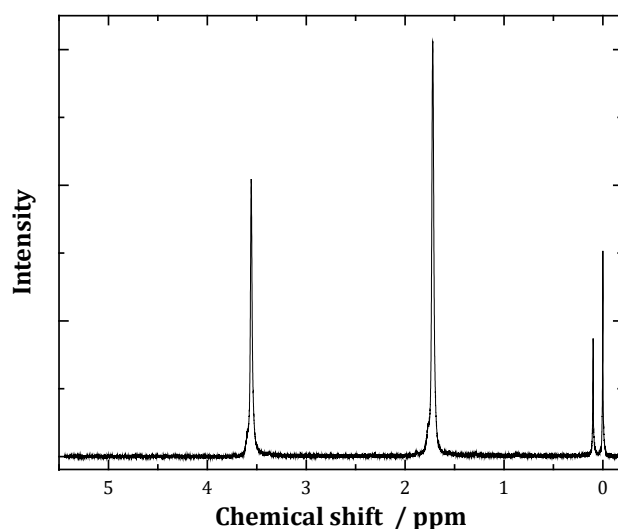


Figure S4. ^1H -NMR spectrum for the supernatant of the sample mixture (in THF- d_8) yielding compound **1**. Tetramethylsilane (TMS) was used as a reference.

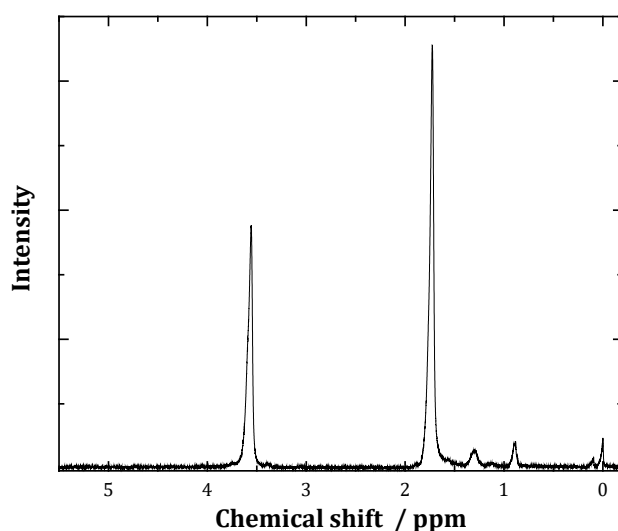


Figure S5. ^1H -NMR spectrum for the supernatant of the sample mixture (in THF- d_8) yielding compound **2**. Tetramethylsilane (TMS) was used as a reference.

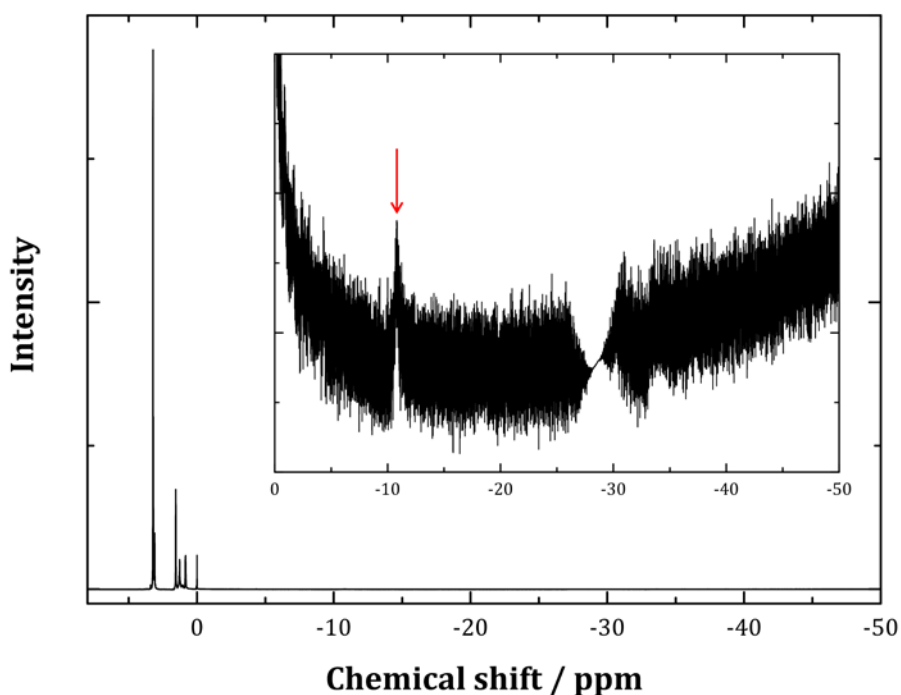


Figure S6. $^1\text{H-NMR}$ spectrum for 20 mg of $\text{NpCl}_4(\text{DME})_2$ dissolved in 0.5 ml of THF-d_8 . Tetramethylsilane (TMS) was used as a reference. Inset figure is the enlargement of the spectrum below 0 ppm, showing a weak but significant peak at around -10.7 ppm (highlighted with a red arrow).

In addition to the signals from free solvent molecules (i.e. DME and THF molecules) above 0 ppm (between 1.5 and 4.0 ppm), the NMR spectrum in Fig. S6 shows a weak but significant peak at around -10.7 ppm (highlighted with a red arrow in the inserted figure). It has been reported that the dissolved species of $\text{NpCl}_4(\text{DME})_2$ in CD_2Cl_2 exhibits $^1\text{H-NMR}$ signals at -1.1 and -41.7 ppm,¹⁴ which are not observed for the spectrum in Fig. S6. As far as we know, the NMR data of the dissolved species of $\text{NpCl}_4(\text{THF})_n$ have not yet been reported. However, the dissolved species of $\text{UCl}_4(\text{THF})_3$, a chemical analogue of $\text{NpCl}_4(\text{THF})_n$, shows a $^1\text{H-NMR}$ signal at -10.5 ppm in toluene- d_8 ,¹⁵ which is comparable to the signal observed at around -11 ppm in Fig. S6. Given these facts, it is reasonable to infer that the DME molecules in the initial $\text{NpCl}_4(\text{DME})_2$ are completely replaced with THF molecules upon the dissolution in THF to form the dissolved species of $\text{NpCl}_4(\text{THF})_n$.

3-5. IR spectroscopy

In addition to the NMR spectroscopy mentioned in the previous section, IR spectroscopy was also applied in order to characterise the sample mixtures yielding compounds **1** and **2**, particularly in terms of the presence/absence of water impurity. Figures S6 and S7 show the IR spectra of the supernatant (left) and solid residue (right) after mixing the two NpCl_4 sources in THF- d_8 . The presence of water by IR spectroscopy is typically confirmed with a strong absorption band associated with the O—H stretching of water molecules above $\sim 3100\text{ cm}^{-1}$. The collected IR spectra, however, show no significant absorption above 3000 cm^{-1} , suggesting that the sample mixtures yielding **1** and **2** did not contain water impurity, also in terms of IR spectroscopy.

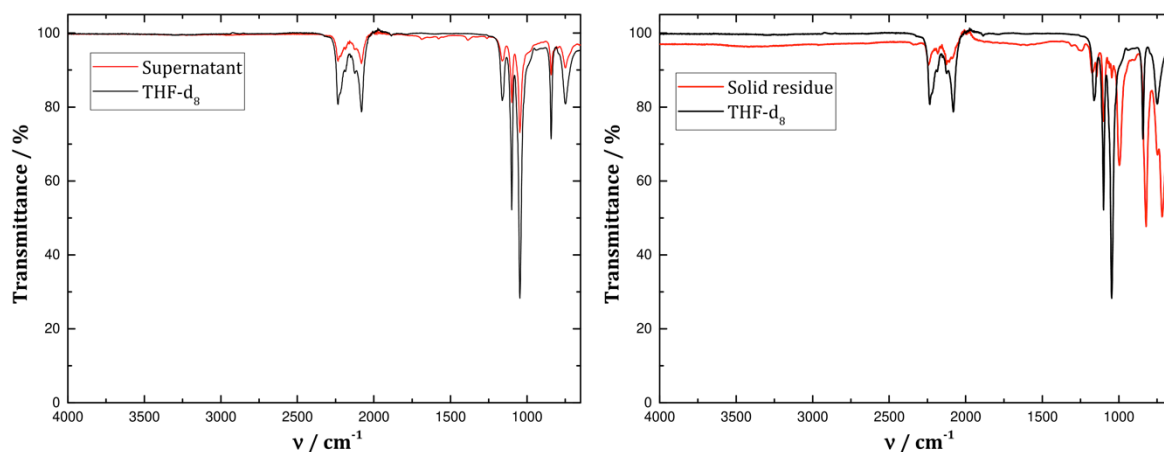


Figure S7. Infrared (IR) spectra for the supernatant (left) and solid residue (right) of the sample mixture (in THF- d_8) yielding compound **1**.

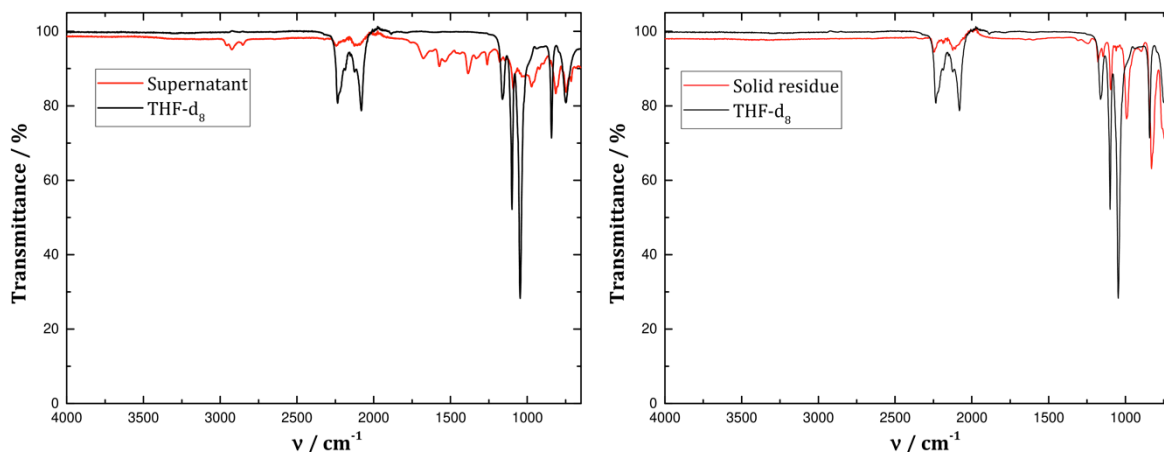


Figure S8. Infrared (IR) spectra for the supernatant (left) and solid residue (right) of the sample mixture (in THF- d_8) yielding compound **2**.

3-6. UV-visible-NIR absorption spectroscopy

As mentioned in Section 1-1, it was practically difficult to estimate the fractions of Np(IV) and - (V) in the starting Np(IV) tetrachloride compounds. For this reason, UV-visible-NIR absorption spectroscopy was employed to estimate the concentrations of Np and the fractions of Np(IV) and - (V) in the sample solutions yielding the compounds **1** and **2**.

First, a solution of 0.011 M Np(IV) was prepared by dissolving pure $\text{NpCl}_4(\text{DME})_2$ in THF, and its UV-visible-NIR absorption spectrum was collected (Fig. S9). The collected spectrum was then compared with the spectrum of 0.011 M Np(IV) that was prepared by dissolving $\text{NpCl}_4(\text{DME})_2$ in DME (Fig. S9). It is obvious that the collected two spectra significantly differs, suggesting that the soluble Np(IV) species in THF is different from those in DME. Together with the NMR result shown in Fig. S6, it is reasonable to conclude that the dissolution of $\text{NpCl}_4(\text{DME})_2$ solid in THF results in the formation of soluble species of $\text{NpCl}_4(\text{THF})_n$ and the coordinated DME molecules in the initial $\text{NpCl}_4(\text{DME})_2$ are completely replaced with THF molecules upon the dissolution.

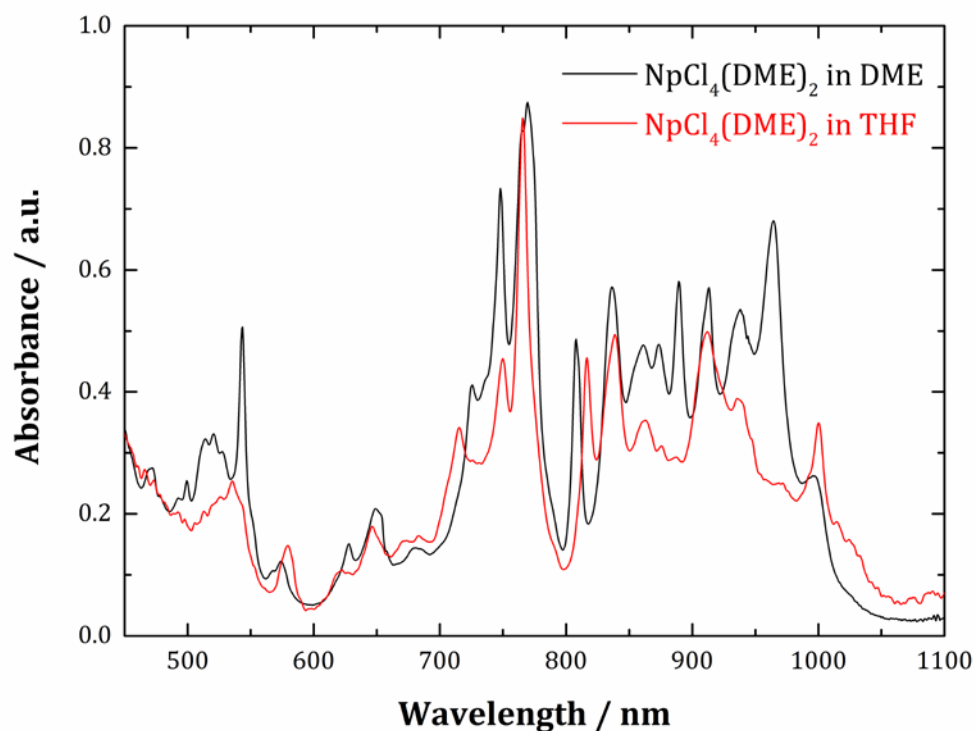


Figure S9. UV-visible-NIR absorption spectra of 0.011 M $\text{NpCl}_4(\text{DME})_2$ dissolved in DME (black) and THF (red) with an optical path length of 1.0 cm.

Second, the collected spectrum was compared with the spectrum of 0.011 M Np(IV) that was prepared by dissolving $\text{NpCl}_4(\text{DME})_2$ in DME (Fig. S10). The intense absorption band observed at 762 nm can be assigned as the strong absorption of Np(IV) species¹⁶ and, therefore, the molar extinction coefficient (ϵ) of Np(IV) in THF can be calculated according to the measured intensity at 762 nm. The value was calculated to be “ $\epsilon_{\text{Np(IV)-THF}} = 90.6 \text{ L/mol}\cdot\text{cm}$ ”.

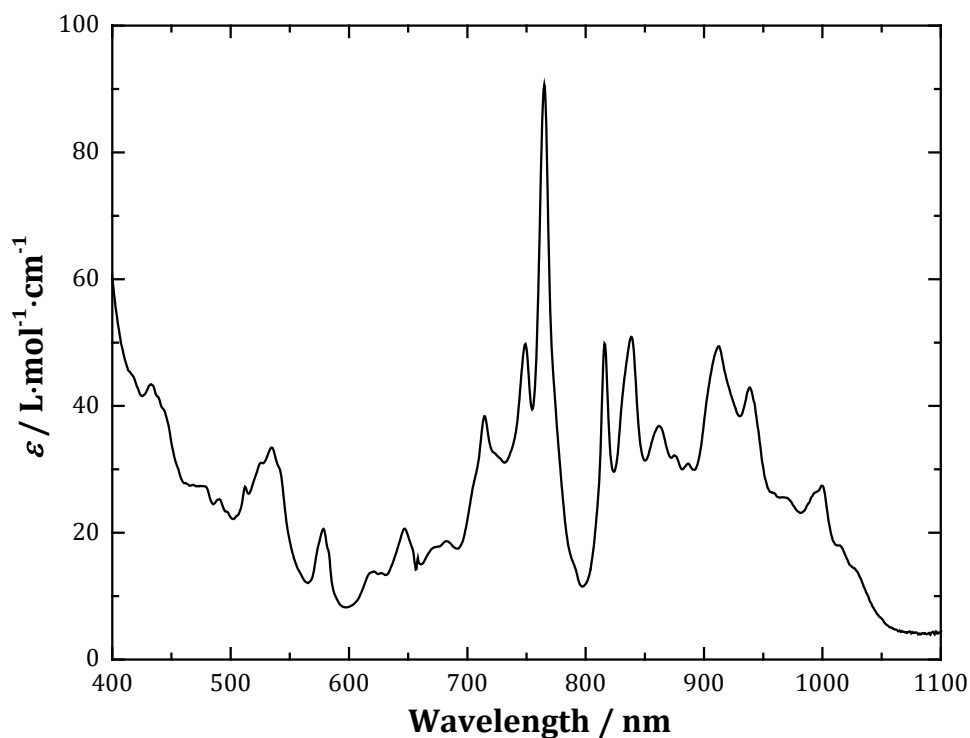


Figure S10. UV-visible-NIR absorption spectrum of 0.011 M $\text{NpCl}_4(\text{DME})_2$ in THF with an optical path length of 1.0 cm. The unit of y -axis is converted to the molar extinction coefficient, ϵ ($\text{L} / \text{mol}\cdot\text{cm}$).

Shown in Fig. S11 are the UV-visible-NIR absorption spectra of the two sample solutions (i.e. supernatants of the sample mixtures) yielding **1** and **2** (hereafter referred to as Solutions **A** and **B**, respectively). Based on the calculated value of $\epsilon_{\text{Np(IV)-THF}}$, the concentrations of Np(IV) in the solutions are estimated to be 0.0026 and 0.0041 M for Solutions **A** and **B**, respectively. Based on the initial amounts of Np source and the volume of the solvent (THF) to prepare Solutions **A** and **B**, the concentrations of Np(V) in the two solutions are further estimated to be 0.0050 and 0.0090 M in Solutions **A** and **B**, respectively. According to these concentration values, the Np(V)/Np(IV) ratios in Solutions **A** and **B** are calculated to be 1.9 and 2.2, respectively. These values confirm that Solution **A** yielding the trinuclear complex **1** (the Np(V)/Np(IV) ratio in the oligomer unit is 2) contained a lower fraction of Np(V) than Solution **B** yielding the tetranuclear complex **2** (the Np(V)/Np(IV) ratio in the oligomer unit is 3).

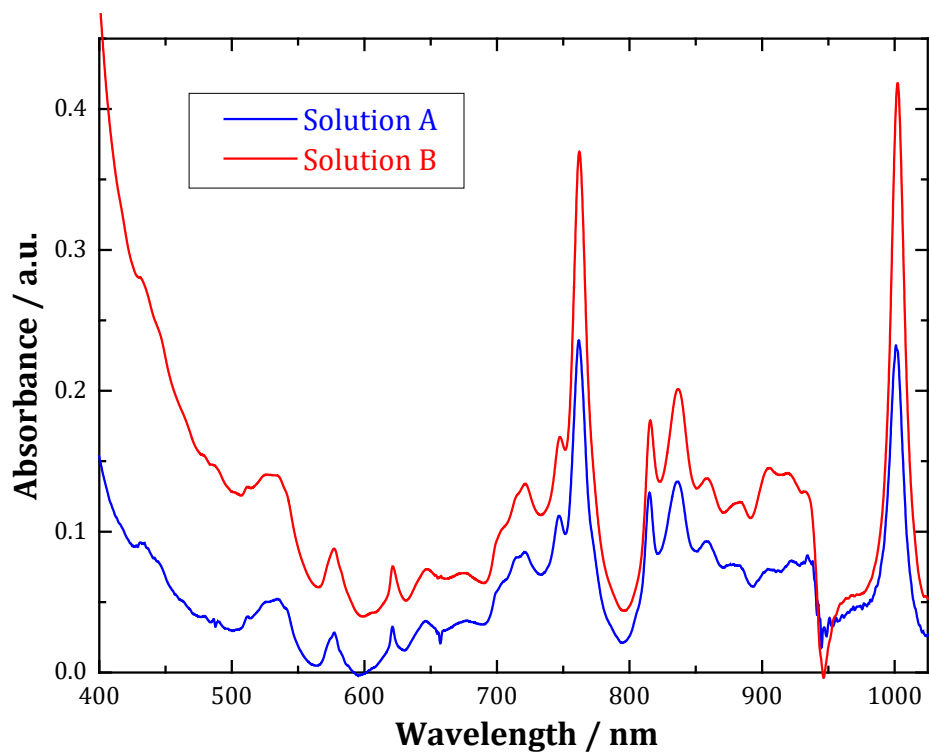


Figure S11. UV-visible-NIR absorption spectra of Solutions **A** and **B** with an optical path length of 1.0 cm.

3-7. PXRD

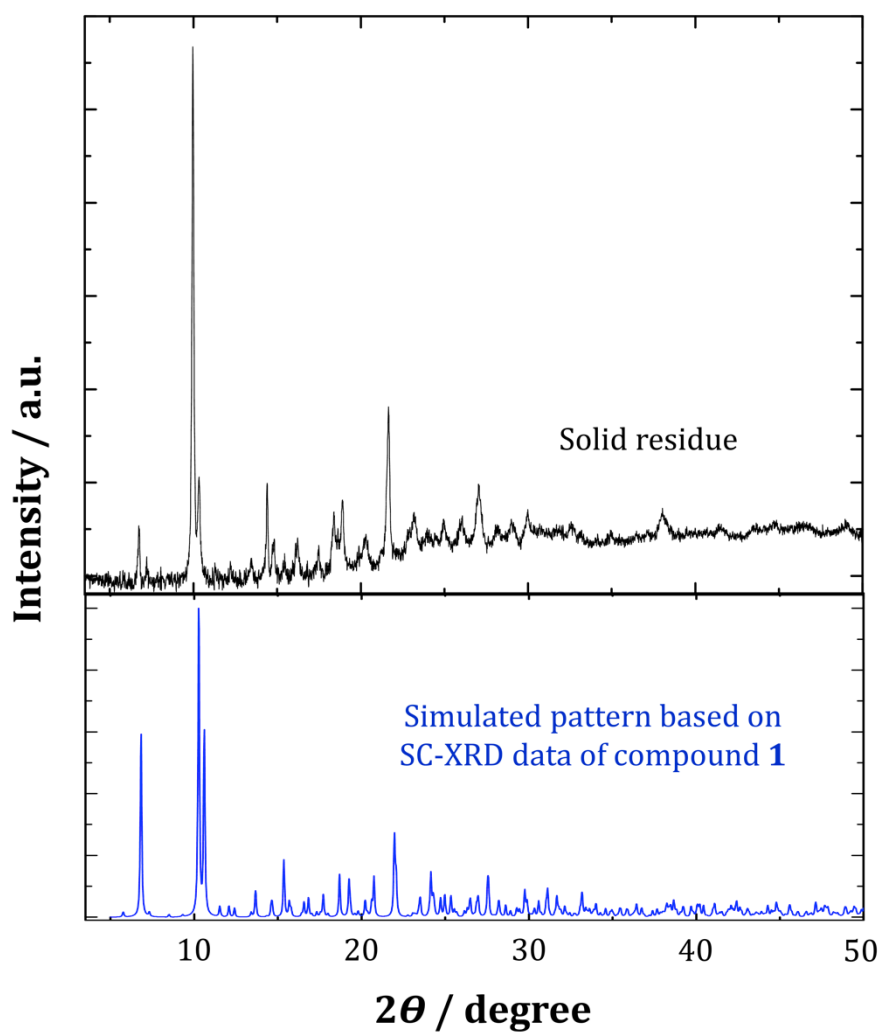


Figure S10. Powder X-ray diffraction profile of the solid residue of the sample mixture yielding compound **1** (top, black line) and simulated pattern based on the SC-XRD structure data of **1** (bottom, blue line), suggesting that the solid residue is primarily composed of **1**. Cu $K\alpha$ radiation.

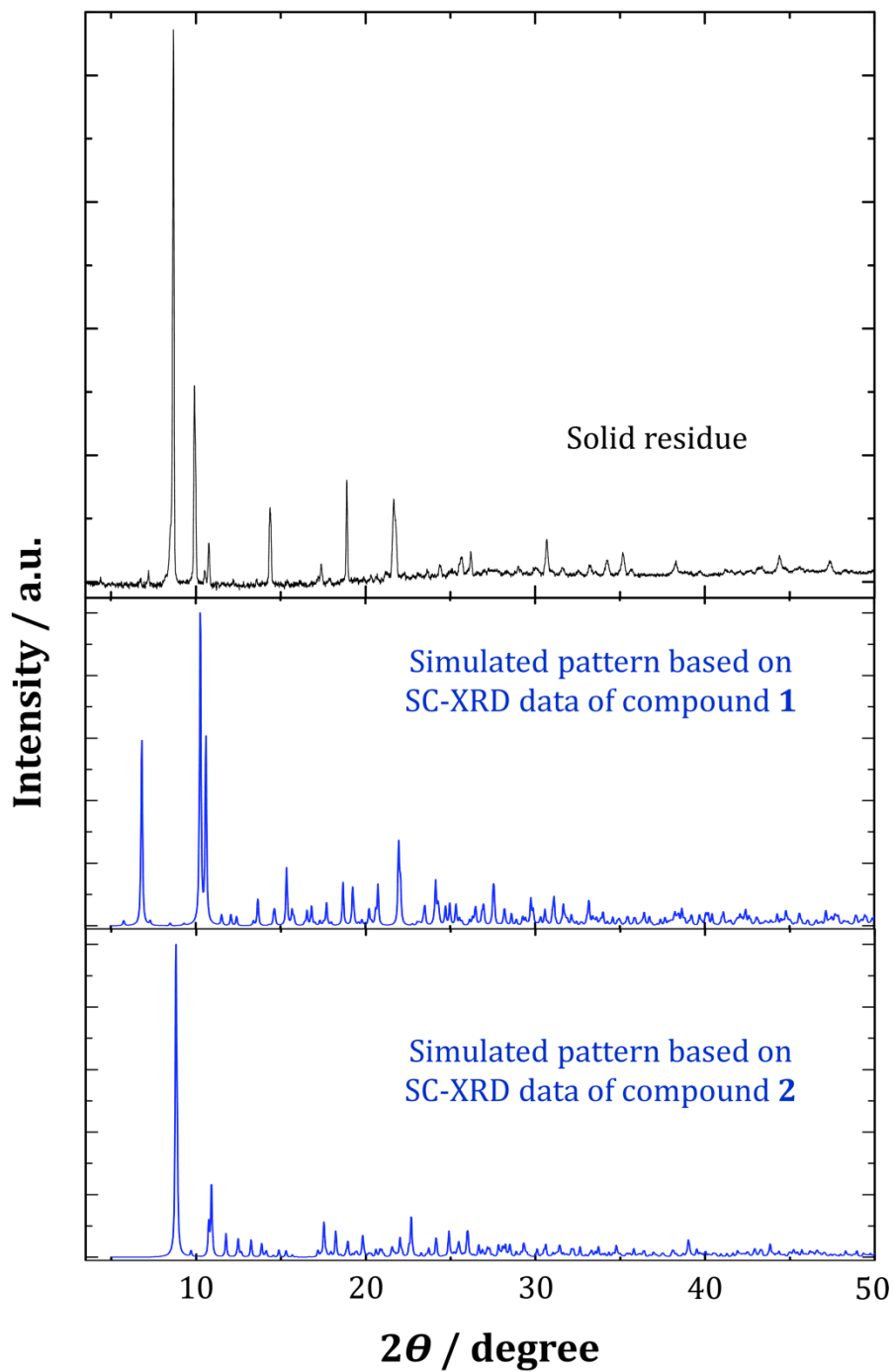


Figure S11. Powder X-ray diffraction profile of the solid residue of the sample mixture yielding compound **2** (top, black line) and simulated patterns based on the SC-XRD structure data of **1** and **2** (bottom, blue lines), suggesting that the solid residue contains **2** as a major phase with **1** as a minor phase and unidentified additional phases. Cu K α radiation.

3-8. Crystallographic data

Table S3. Crystallographic data and structure refinement details for compounds **1** and **2**

	1	2
Empirical formula	C ₂₈ H ₅₆ Cl ₆ Np ₃ O ₁₁	C ₂₄ H ₄₈ Cl ₇ Np ₄ O ₁₂
CCDC number	1884777	1884778
M (g/mol)	1492.42	1724.77
Crystal system	monoclinic	monoclinic
Space group	<i>P</i> 2 ₁ / <i>c</i>	<i>C</i> 2/ <i>c</i>
<i>a</i> (Å)	15.3447(17)	15.009(4)
<i>b</i> (Å)	24.156(3)	14.159(3)
<i>c</i> (Å)	11.5292(8)	40.069(9)
α (deg)	90	90
β (deg)	90.060(3)	91.406(2)
γ (deg)	90	90
<i>V</i> (Å³)	4273.5(7)	8513.(3)
<i>T</i> (K)	100.(2)	100.(2)
<i>Z</i>	4	8
ρ_{calcd} (Mg/m³)	2.320	2.692
Abs coeff (mm⁻¹)	7.664	10.173
θ_{max} (deg)	27.880	23.2596
<i>R</i> [<i>I</i> > 2σ(<i>I</i>)]^a	0.0207	0.1402
<i>wR</i>2(int)^a	0.0382	0.3249
<i>w</i> scheme <i>d, e</i>	0.0103, 8.3544	0.0001, 6904.4883
Data/param	10184/433	6089/418
Res. Dens (eÅ⁻³)	1.294, -1.101	6.554, -5.350
<i>R</i>_{int}	0.0334	0.0596
Goof	1.072	1.358

$$^a w = 1/[\sigma^2(F_o^2) + (dP)^2 + eP] \text{ where } P = (F_o^2 + 2F_c^2)/3$$

References

1. D. Patel, A. J. Wooles, E. Hashem, H. Omorodion, R. J. Baker and S. T. Liddle, *New J. Chem.*, 2015, **39**, 7559-7562.
2. Bruker, *APEX3*, (2016) Bruker AXS Inc., Madison, Wisconsin, USA.
3. G. M. Sheldrick, *SADABS*, (1996) University of Göttingen, Göttingen, Germany.
4. G. M. Sheldrick, *Acta Crystallogr.*, 2015, **A71**, 3-8.
5. C. B. Hubschle, G. M. Sheldrick and B. Dittrich, *J. Appl. Crystallogr.*, 2011, **44**, 1281-1284.
6. S. M. Cornet, L. J. Haller, M. J. Sarsfield, D. Collison, M. Helliwell, I. May and N. Kaltsoyannis, *Chem. Commun.*, 2009, 917-919.
7. I. Charushnikova, E. Bosse, D. Guillaumont and P. Moisy, *Inorg. Chem.*, 2010, **49**, 2077-2082.
8. I. D. Brown, *Chem. Soc. Rev.*, 1978, **7**, 359-376.
9. T. E. Albrecht-Schmitt, P. M. Almond and R. E. Sykora, *Inorg. Chem.*, 2003, **42**, 3788-3795.
10. T. Z. Forbes, C. Wallace and P. C. Burns, *Can. Mineral.*, 2008, **46**, 1623-1645.
11. O. C. Gagne and F. C. Hawthorne, *Acta Crystallogr.*, 2015, **B71**, 562-578.
12. W. H. Zachariasen, *J. Less-Common Metals*, 1978, **62**, 1-7.
13. G. R. Fulmer, A. J. M. Miller, N. H. Sherden, H. E. Gottlieb, A. Nudelman, B. M. Stoltz, J. E. Bercaw and K. I. Goldberg, *Organometallics*, 2010, **29**, 2176-2179.
14. S. D. Reilly, J. L. Brown, B. L. Scott and A. J. Gaunt, *Dalton Trans.*, 2014, **43**, 1498-1501.
15. W. G. Van der Sluys, J. M. Berg, D. Barnhardt and N. N. Sauer, *Inorg. Chim. Acta*, 1993, **204**, 251-256.
16. A. Ikeda-Ohno, C. Hennig, A. Rossberg, H. Funke, A. C. Scheinost, G. Bernhard and T. Yaita, *Inorg. Chem.*, 2008, **47**, 8294-8305.